Hydrogel-polyurethane Interpenetrating Network Material as an Advanced Draw Agent for Forward Osmosis Process

Jing Wei[1], Ze-Xian Low[1], Ranwen Ou[1], George P Simon[2], Huanting Wang*[1]

[1]Department of Chemical Engineering, Monash University, Clayton, Victoria 3800, Australia
[2]Department of Materials Engineering, Monash University, Clayton, Victoria 3800, Australia

*Corresponding author: E-mail: huanting.wang@monash.edu

Abstract

Water desalination and purification are critical to address the global issue of the shortage of clean water. Forward osmosis (FO) desalination is an emerging low-cost technology for clean water production from saline water. The lack of a suitable draw agent is one of hurdle for the commercialization of FO desalination technology. Recently, the thermoresponsive hydrogel has been demonstrated to be a potential draw agent for the FO process. However, the commonly used hydrogel powder shows a much lower flux than other kind of draw agent such as inorganic salts. In this work, a hydrogel-polyurethane interpenetrating network (HPIPN) with monolith form was prepared by controlling the radical polymerization of the monomers (N-isopropylacrylamide and sodium acrylate) in the macropores (~ 400 μm) of commercial polyurethane foam (PUF). These HPIPN composites show a flux as high as 17.9 LMH, which is nearly 8 times than that of hydrogel powders (2.2 LMH). The high flux is attributed to the 3-D continuous hydrogel-polyurethane interpenetrating network, which can effectively enhance the water transport inside the monolith.

Keywords: Hydrogel; forward osmosis; desalination; water transport; draw agent

1. Introduction

Water desalination and purification are critical to address the global issue of the shortage of clean water (Patel-Predd, 2006; Subramani et al, 2015; Akther et al, 2015). The applications of membrane-based technique such as nanofiltration (NF), reverse osmosis (RO), membrane distillation (MD), and forward osmosis (FO) are widely used to solve the scarcity of fresh water. Forward osmosis, using the osmotic pressure difference as the driving force to draw the clean water from saline water through a semi-permeable membrane, has been recognized in recent years as an attractive process for water desalination and treatment, because it has the potential to achieve reduced process costs by directly using other types of energy such as low-grade heat, reduced fouling propensity, and is easy to clean (Cath et al, 2006; McCutcheon et al, 2005; Gormly et al 2011; Hoover et al, 2011; Lutchmiah et al, 2011; Chung et al, 2012). Although the FO technology has attracted increasing attentions in water treatment, one of the main obstacles is the lack of high-performance draw solute (Chekli et al, 2012; Ge et al, 2013; Li et al, 2013). It is very challenging to develop an ideal draw agent with a high osmotic pressure, easy and fast regeneration without significant loss of draw agent, and non-toxicity. Much research has focused on new draw agents such as inorganic salts, functionalized magnetic nanoparticles, and thermoresponsive polyelectrolyte solutions (McCutcheon et al, 2005; Achilli et al, 2010; Ling et al, 2010; Xu et al, 2010; Yen et al, 2010; Bai et al, 2011; Ge et al, 2011; Ling et al, 2011; Ge et al, 2012; Sarp et al, 2012; Alnaizy et al, 2013; Cai et al, 2013; Cai et al, 2013; Ge et al, 2013).

Our group has recently reported for the first time, the use of a stimuli-responsive polymer hydrogel as the draw agent in FO desalination (Li et al, 2013; Li et al, 2011; Li et al, 2011; Li et al, 2013; Ou et al, 2013; Razmjou et al, 2013; Razmjou et al, 2013; Razmjou et al, 2013; Zeng et al, 2013; Wang et al, 2014). Hydrogels with three-dimensional networks of polymer chains and abundant hydrophilic groups can entrap large volumes of water due to their

relative higher osmosis pressure, and are thus widely used as scaffolds for tissue engineering, as temporary supports for cells and as vehicles for drug delivery systems. Important is the fact that stimuli-responsive polymer hydrogels can undergo a reversible swelling change in response to external environmental stimuli. For example, poly(N-isopropylacrylamide) (PNIPAM)-based hydrogels show a lower critical solution temperature (LCST) at about 32 ^{o}C, which can change from hydrophilic to hydrophobic above their LCST and release the entrapped water from their network. This intrinsic property can be applied for the dewatering of hydrogel after FO desalination, thus exhibiting an energy-efficient method to regenerate the draw agent. Although the hydrogel has been proved to be a potential draw agent, there are still many issues to be solved, such as low flux, and low yield for clean water. To date the hydrogel has usually been used in the powder form, with the particle size ranging from 2 - 1000 μm. As the hydrogel particle size decreases, the contact area between hydrogel and FO membrane increases remarkably, resulting in an enhanced FO flux (Razmjou et al, 2013; Hartanto et al, 2015; Zhang et al, 2015; Ali et al, 2015). At the same time, increasing the amount of draw agent will give an enhanced flux but this does not increase indefinitely with more hydrogel. This is because the water transport from the first layer hydrogel particles contacted with FO membrane to the other layers becomes difficult. Due to this transport barrier, the hydrogel powder shows a lower flux compared to the common used draw agent such as inorganic salts. It is urgent to solve the transport problem for the hydrogel draw agent and further increase the flux, if this approach is to be further used.

Another drawback for the hydrogels is their weak mechanical toughness. After swelling, the hydrogel can be easily broken when handled during application. In order to improve their mechanical properties, researchers reported the synthesis of polymer hydrogel/polyurethane foam (PUF) composites (Liu et al, 2008; Teramoto et al, 2014). As the PUF shows 3-D macroporous structure; it is a good candidate to accommodate the hydrogel. At the same time,

the plastic scaffold can also enhance the mechanical properties of hydrogel and make it easier to handle. However, the performance of foam-infiltrated hydrogels as the draw agent material in forward osmosis has never been yet investigated.

In this work, a hydrogel-polyurethane interpenetrating network (HPIPN) with monolith form was prepared by controlling the radical polymerization of the monomers (N-isopropylacrylamide and sodium acrylate) in the macropores (~ 400 μm) of commercial polyurethane foam (PUF). By tailoring the shape of PUF, the HPIPN can be easily shaped. The swollen PUF/hydrogel can be easily handled during the application and shaped even by scissors, without destroying their monolithic shape. The content of hydrogel in the PUF/hydrogel composites can be easily adjusted from 50 to 89 wt% by increasing the concentration of monomers from 12.6 to 20 wt %. These PUF/hydrogel composites were used as draw agents for forward osmosis desalination, and we were able to demonstrate a high flux from 3.9 to 17.9 LMH as the content of hydrogel in the composites from 50 to 89 wt%. By comparison, the flux was only 2.2 LMH when hydrogel powders were used as the draw agent. The high flux is attributed to the 3-D continuous hydrogel-polyurethane interpenetrating network, which can effectively enhance the water transport inside the monolith.

2. Experimental Section

2.1 Chemicals and Materials: Sodium acrylate (SA, 99 %), N, N'-methylenebisacrylamide (MBA, 99 %), N-isopropylacrylamide (NIPAM, 96 %) and ammonium persulfate (98 %) were purchased from Sigma-Aldrich Australia. Forward osmosis (FO) membranes made from cellulose triacetate with an embedded polyester screen mesh were provided by Hydration Technologies Inc. (Albany, OR).

2.2 Preparation of Hydrogel Draw Agent

The poly(N-isopropylacrylamide)-*co*-poly(sodium acrylate) (PNIPAM-*co*-PSA) hydrogel powders were prepared via radical polymerization by using NIPAM and SA as monomers, MBA as a cross-linker, and ammonium persulfate (APS) as an initiator. Typically, 3.33 g of SA and 1.67 g of NIPAM were dissolved in 25 ml of deionized water at room temperature. Then, 0.12 g of MBA and 0.08 g of APS were added into the above solution. After complete dissolution, the polymerization was carried out at 90 ^{o}C for 2 h. To remove the unreacted monomers and low-molecular-weight polymer, the hydrogels were cut into small pieces and immersed into deionized water at room temperature for 3 days. The hydrogel was then dried at 80 ^{o}C in an oven and the powder form obtained by grinding dried hydrogel with a mortar and pestle.

To prepare PNIPAM-PSA-PU composited hydrogels, the polyurethane foam (PUF) of tailored macro-size was fully soaked in a clear solution of monomers, cross-linker and initiator. The PUF was squeezed using spatulas to exclude the air in the foam. The saturated PUF and residual precursor were heated to 90 ^{o}C to cause polymerization. The hydrogel outside of the PUF was carefully scraped before soaking in EtOH and water mixture (v/v, 1:1), to remove the unreacted monomers and low-molecular-weight polymer. The PNIPAM-PSA-PU composite hydrogel was obtained after being dried at 80 ^{o}C in an oven. The mass ratio of PUF and hydrogel was calculated by determining the mass of PUF before and after loading hydrogel. The mass ratio of gel respect to PUF (from 1:1 to 8:1) was adjusted by changing the concentration of monomers solution from 12.6 to 20 wt%.

2.3 Characterization

The Scanning Electron Microscopy (SEM) image of PUF and PNIPAM-PSA-PU composited hydrogel was determined by field-emission scanning electronic microscopy (FEI Nova NanoSEM 450). The sample was sputter-coated with platinum before imaging.

FO measurements were carried out in a home-made setup, as previously reported (Zeng et al, 2013). The dried hydrogel monoliths with size of about 0.5×0.5×1 cm as a draw agent were placed on the active side of the FO membrane with an effective area of 4.90 cm^2, while DDI water or NaCl solution with different concentrations (0.2 - 3.5 wt %) were used as the feed solution on the upstream side of the FO membrane. The FO membrane was immersed in DDI water for at least 12 h before use. Water flux, F (L m^{-2} h^{-1}, or LMH), was calculated by

$$F = \frac{V}{At}$$

where V (L) is the volume of water absorbed by the hydrogel, calculated by dividing the mass of the water (i.e., the mass increase of the hydrogel measured by a KERN ASL256-4A balance, Germany, accuracy: 0.1 mg) by its density, t (h) is the time and A (m^2) is the effective area of the FO membrane (4.90 cm^2).

The swelling experiment was carried out by soaking the monolith with the same size (about 1×1×1.5 cm) in 500 ml of DI water. The mass of sample was recorded at intervals after carefully wiping the water adsorbed on the surface of monolith with tissue. To visually investigate the water transport inside the dry hydrogel/PUF, copper nitrate solution was used. Typically, 0.6 g of $Cu(NO_3)_2 \cdot 3H_2O$ was dissolved in 50 mL of water. Then the solution was poured in a petri dish to obtain a solution of around 3 mm depth. The dry hydrogel/PUF monolith stood in the solution to contact with the solution adequately. The colour of dry hydrogel/PUF monolith was recorded via photos.

In the solar dewatering process, 0.76 g of dry hydrogel PNIPAM-PSA-PU composites with different swelling ratios (100, 200, 420 wt%) were placed under the sunlight simulator (2 kW/ m^2). The water recovery rate (R) was calculated by

$$R = \frac{W_1}{W_0} \times 100\%$$

where W_l is the weight of the water lost during the solar dewatering and W_0 is the weight of the water contained in the swollen hydrogel before the dewatering test.

3 Results and Discussion

3.1 Synthesis and characterization of hydrogel/PUF composites

PUF is one of most commonly-used, commercial polymer foams and it shows high porosity, has an open framework, and thus high flexibility. PUF was fully soaked in the precursors of hydrogel to allow the monomers enter the macropores of PUF and polymerize in the PUF (**Figure 1**, Step 1). The polymer hydrogel, poly(N-isopropylacrylamide)-*co*-poly(sodium acrylate) (PNIPAM-*co*-PSA), was chosen as the composition of a typical hydrogel draw agent we have often used (Li et al, 2011; Li et al, 2011). The PNIPAM segment is thermally-responsive, which undergoes a reversible phase separation as the temperature reaches above its lower critical solution temperature (LCST, ~ 32 ^{o}C). When the temperature increases up to 32 ^{o}C, the PNIPAM changes from hydrophilic to hydrophobic. The trapped water can be easily recovered, which is crucial for thermal dewatering after FO process. However, the swelling pressure for this nonionic polymer hydrogel is low, and thus a low FO flux was obtained (Li et al, 2011; Li et al, 2011). The incorporation of ionic segment (PSA) can effectively increase the overall swelling pressure of the resulting copolymer and the flux of FO process (Wack et al, 2009; Li et al, 2011; Ali et al, 2015). Due to the random copolymerization process, the PSA and PNIPAM segments are distributed randomly throughout the polymer network. After washing and drying to remove the unreacted monomers and water (Figure 1, Step 2), the dry hydrogel/PUF composites were obtained.

As the commercial polyurethane foam (PUF) shows high flexibility, it can be easily tailored to any shape for different applications (**Figure 2**a). After loading the precursors of hydrogel including monomers (SA, NIPAM), crosslinker (N, N'-methylenebisacrylamide; MBA) and

initiator (ammonium persulphate; APS) in water followed by radical polymerization at 90 ^{o}C, hydrogel/PUF composites with similar shape and size were obtained (Figure 2b). After washing with ethanol and water to remove the unreacted monomers, the composites were fully dried in the oven. The obtained dry hydrogel/PUF showed a similar shape to the PUF, but clear shrinkage was apparent in the six faces of cube, which is caused by the removal of water (~ 80 wt %) from the hydrogel (Figure 2c). Due to the uniform distribution of the hydrogel in the PUF matrix, the shape of hydrogel/PUF composites could be retained well, even after handling and shaping (Figure 2d-f), which indicates a robust mechanical structure.

SEM images of PUF show that it has 3-D continuous porous structure with pore size of about 400 µm (Figure 3a). After loading the hydrogel, SEM image of hydrogel/PUF (mass ratio, 1:1) reveals that the hydrogel has been successfully loaded into the macropores of PUF (Figure 3b). As the mass ratio of hydrogel with respect to PUF further increases from 4:1 to 8:1, almost all of the macropores are filled with hydrogel (Figure 3c-d), indicating the formation of the hydrogel/polyurethane interpenetrating network (HPIPN). From the results of hydrogel/PUF (Figure 2b), the hydrogels were distributed uniformly in the PU foam. After drying, the dry hydrogels remained within the PUF, which reveals homogenous shrinkage of both hydrogel and PUF. As one of most common sponges, PUF is elastic. Due to the uniform distribution of hydrogel in PU foam, the shrinkage of hydrogel during drying process encourages the shrinkage of the PUF. This may be due to strong hydrogen bonding between polyurethane and poly(N-isopropylacrylamide), which can effective avoid a phase separation of PUF and polymer hydrogel during the polymerization and drying process. The optical images (Figure 2) also confirm that the overall homogeneous nature of hydrogel distribution at a centimetre-scale after polymerization and drying process.

3.2 Swelling property

To investigate the water adsorb kinetics of hydrogel/PUF, the hydrogel/PUF (mass ration, 8:1) was immersed in DDI water. It can be seen that the hydrogel/PUF material shows a rapid rate of water adsorption (Figure S1). During this adsorption, the volume of the hydrogel/PUF also increases, as shown in Figure S2a. From the optical image of the dry and swollen hydrogel/PUF, the cuboid shape of the composites remains almost constant, albeit a change in volume. In the middle area of hydrogel/PUF bulk, the colour is yellow, which is similar to the dry one, indicating the water enters the matrix of composites from outside to inside gradually. It is important to investigate the nature and mechanism of water transport in the hydrogel/PUF matrix. To achieve this, one end of the dry hydrogel/PUF was placed in the copper nitrate solution to allow the solution transport from the bottom to the upper layer of hydrogel/PUF (Figure S2b). The optical images clearly show that water is readily transported from the bottom to top of composites. From the colour differences, it can be thus concluded that water can readily transport from the surface of composites inwards.

As the size of the bulk materials plays a key role during water transport inside of the hydrogel, hydrogel/PUF composites with different ratios of hydrogel to PUF, but of a similar external size (i.e. 1×1×1.5 cm) were immersed in water to investigate the water absorption kinetics. As seen from Figure 4a, the composites with high hydrogel content show an enhanced water absorption rate, due to the high swelling ratio of hydrogel materials.

3.3 Water flux in the FO process

The hydrogel/PUF composites were further used as the draw agent due to their 3-D continuous structure and fast rate of water adsorption and transport. The setup for the test of FO process is shown in Figure 4b. The solid draw agent (hydrogel/PUF) was put on the active side of FO membrane, with the support layer of FO membrane facing the feed solution. The DDI water was first chosen as the feed solution. When pure PUF was used as the draw

agent, no flux was observed due to its weak capillary force. When hydrogel powder was used as the draw agent, the 1h's flux is as low as 2.2 LHM, which is consistent to previous reports (Zeng et al, 2013). Since the water is difficult to transport from the bottom to the up layer of draw agent, the up layer of the hydrogel is dry after 8 h's FO process. Conversely, when hydrogel/PUF composites were used as the draw agent, the water can easily transport from the bottom to the top layer of the draw agent. This is important to the draw agent, as all the draw agent can be effectively used during the FO process. When the mass ratio of hydrogel respect to PUF increases from 1:1 to 8:1, the flux (1 hour) also increases from 3.9 to 17.9 LMH (Figure 4c). When the hydrogel was fully filled in the pores of PUF, the flux is highest, which is almost 8 times that of the commonly-used hydrogel powders without PUF. PNIPAM hydrogel powder and PNIPAM/PUF were also used as draw agents, and the result showed the incorporation of PUF into PNIPAM also increased the water flux significantly (Figure S3). In addition, PSA-*co*-PNIPAM hydrogel powder (or monolith) showed higher flux than PNIPAM hydrogel powder (or monolith), indicating that the incorporation of SA into the polymer hydrogel can effectively increase the swelling pressure of the composite hydrogel. This is consistent with the previous report (Li et al, 2011). All these results show that the FO flux can be greatly improved by loading hydrogel into the PUF matrix. As the PUF does not have a good swelling pressure, it only acts as a 3D continuous and elastic scaffold. But PUF incorporation improves water transport through the polymer hydrogel, thus enhancing the swelling pressure of draw agent.

Due to its high flux, hydrogel/PUF with mass ration of 8:1 was further used as the draw agent and different concentrations of sodium chloride solution were used as the feed solution. As the concentrations of NaCl solution increases from 0.2 to 3.5 wt%, the one hour's flux decreases from 14.8 to 4.2 LMH, due to the higher osmotic pressure of feed solution with

higher concentration of NaCl solution (Figure 4d). This flux is better than all the previous reported hydrogel draw agents (Table S1).

Base on the above results, the high flux was ascribed to the unique hydrogel-polyurethane interpenetrating network with a 3D continuous structure. During the FO process, the osmotic pressure (swelling pressure) of the draw agent is very important to the FO flux. The ionic hydrogel shows high swelling pressure, which can draw water across the FO membrane more effectively. For example, poly(acrylic acid)/poly(sodium acrylate) copolymer hydrogels with polymer volume fractions between 0.03 and 0.30 exhibit a swelling pressure ranging from 0.20-4.23 MPa (Wack et al, 2009). This value is even greater than the osmotic pressure of seawater (2.34 MPa at 25 ^{o}C, salt concentration of 35 g/L). However, the FO flux induced by hydrogel draw agents is usually low because the water diffusion and transport in the hydrogel is not as good as the liquid draw solution. When the draw solution was used, stirring can be used to effectively eliminate the concentration gradient. However, when "solid" hydrogel draw agent was used, the concentration gradient in the hydrogel is difficult to be eliminated as water becomes trapped in the hydrogel particles and is difficult to transport between different hydrogel particles (**Figure 5**a). As a result, only the hydrogel particles on the active surface of FO membrane can be effectively utilized. The hydrogel particles far away from the membrane surface were still dry after the FO process. We demonstrate here that the unique hydrogel-polyurethane interpenetrating network with a 3D continuous structure can effectively solve this problem, as the water can readily transport inside the hydrogel/PUF composite. As the hydrogel in the matrix of the hydrogel/PUF composites is continuous, the hydrogel can easily pull the water from the bottom to the top layer (Figure 5b). In addition, it is likely that there may be an interface between hydrogel and PUF surface, which can produce a strong capillary force and provide a transport pathway to speed the water transport inside the hydrogel/PUF composite.

3.4 Dewatering

In the dewatering process, the hydrogel/PUF composites with different swelling ratios (100, 200 and 420 wt%) were heated under the concentrated sunlight with an intensity of 2.0 kW m^{-2} (**Figure 6**a). During the solar dewatering process, a portion of water may evaporate as vapor. After exposure to the simulated sunlight for 90 min, the water released from swollen hydrogel/PUF composites is around 79, 75, 46 wt% for swelling ratios 100, 200 and 420% respectively. As the water content in the swelling hydrogel/PUF composite increases from 100 to 200 wt%, their water recovery is similar, indicating that the water adsorbed by hydrogel/PUF composites can be easily removed. When the swelling ratio increases to 420 wt%, the high water content makes the temperature of composites increase slowly, resulting in a lower recovery rate.

Under the same dewatering condition, the water inside the PNIPAM/PUF composite was easily released when the temperature increased to 32 ^{o}C (Figure S4). Nearly 51 wt% of water inside PNIPAM/PUF composites was recovered after 20 min heating, and the dewatering flux was 4.5 LMH. For the PSA-*co*-PNIPAM/PUF composites, 11 wt% of water was recovered and the dewatering flux was 1.1 LMH. As shown in the temperature of PSA-*co*-PNIPAM/PUF composite versus time curves, the temperature of samples reached 32 ^{o}C after 20 min heating; this is because the incorporation of ionic PSA polymer in the hydrogel can effectively increase the FO flux due to its higher swelling pressure. However, PSA can also decrease the dewatering flux as PSA is not thermally responsive.

4. Conclusion

A hydrogel-polyurethane interpenetrating network (HPIPN) with a monolith form was prepared by controlling the polymerization of the monomers (N-isopropylacrylamide and sodium acrylate) in the macropores (~ 400 μm) of commercial polyurethane foam. By

tailoring the shape of PUF, the result HPIPN can be easily shaped on an engineering scale. The content of hydrogel in the HPIPN can be adjusted from 50 to 89 wt% by increasing the concentration of monomers from 12.6 to 20 wt %. The HPIPN was further used as draw agent for forward osmosis desalination, which shows high flux from 3.9 to 17.9 LMH as the content of hydrogel in the composites from 50 to 89 wt%. Such a high flux is attributed to the 3-D continuous hydrogel-polyurethane interpenetrating network, which can effectively enhance the water transport inside the monolith.

5. Acknowledgments

This work is supported by the Baosteel-Australia Research and Development Centre (BAJC) (BA13005) and the Australian Research Council (Linkage Project No.: LP140100051).

6. References

Patel-Predd, P. 2006, Water desalination takes a step forward. Environ. Sci. Technol. 40(11), 3454-3455.

Subramani, A., Jacangelo, J. G. 2015, Emerging desalination technologies for water treatment: A critical review. Water Res., 75, 164-187.

Akther, N., Sodiq, A., Giwa, A., Daer, S., Arafat, H. A., Hasan, S.W. 2015, Recent advancements in forward osmosis desalination: A review. Chem. Eng. J. 281 502-522.

Cath, T. Y., Childress, A. E., Elimelech, M. 2006, Forward osmosis: Principles, applications, and recent developments. J. Membr. Sci. 281(1-2), 70-87.

McCutcheon, J. R., McGinnis, R. L., Elimelech, M. 2005, A novel ammonia-carbon dioxide forward (direct) osmosis desalination process. Desalination 174(1), 1-11.

331 Gormly, S., Herron, J., Flynn, M., Hammoudeh, M., Shaw, H. 2011, Forward osmosis for
332 applications in sustainable energy development. Desalination and Water Treatment 27 (1-3),
333 327-333.

334 Hoover, L. A., Phillip, W. A., Tiraferri, A., Yip, N. Y., Elimelech, M. 2011, Forward with
335 Osmosis: Emerging Applications for Greater Sustainability. Environ. Sci. Technol. 45 (23),
336 9824-9830.

337 Lutchmiah, K., Cornelissen, E. R., Harmsen, D. J. H., Post, J. W., Lampi, K., Ramaekers, H.,
338 Rietveld, L. C., Roest, K. 2011, Water recovery from sewage using forward osmosis. Water
339 Sci. Technol. 64(7), 1443-1449.

340 Chung, T.-S., Zhang, S., Wang, K. Y., Su, J., Ling, M. M. 2012, Forward osmosis processes:
341 Yesterday, today and tomorrow. Desalination 287, 78-81.

342 Chekli, L., Phuntsho, S., Shon, H. K., Vigneswaran, S., Kandasamy, J., Chanan, A. 2012, A
343 review of draw solutes in forward osmosis process and their use in modern applications.
344 Desalination and Water Treatment 43(1-3), 167-184.

345 Ge, Q., Ling, M., Chung, T.-S. 2013, Draw solutions for forward osmosis processes:
346 Developments, challenges, and prospects for the future. J. Membr. Sci. 442, 225-237.

347 Li, D., Wang, H. 2013, Smart draw agents for emerging forward osmosis application. J.
348 Mater. Chem. A 1(45), 14049-14060.

349 Achilli, A., Cath, T. Y., Childress, A. E. 2010, Selection of inorganic-based draw solutions
350 for forward osmosis applications. J. Membr. Sci. 364(1-2), 233-241.

Ling, M. M., Wang, K. Y., Chung, T.-S. 2010, Highly Water-Soluble Magnetic Nanoparticles as Novel Draw Solutes in Forward Osmosis for Water Reuse. Ind. Eng. Chem. Res. 49(12), 5869-5876.

Xu, Y., Peng, X., Tang, C. Y., Fu, Q. S., Nie, S. 2010, Effect of draw solution concentration and operating conditions on forward osmosis and pressure retarded osmosis performance in a spiral wound module. J. Membr. Sci. 348(1-2), 298-309.

Yen, S. K., Haja N, F. M., Su, M., Wang, K. Y., Chung, T.-S. 2010, Study of draw solutes using 2-methylimidazole-based compounds in forward osmosis. J. Membr. Sci. 364(1-2), 242-252.

Bai, H., Liu, Z., Sun, D. D. 2011, Highly water soluble and recovered dextran coated Fe_3O_4 magnetic nanoparticles for brackish water desalination. Sep. Purif. Technol. 81(3), 392-399.

Ge, Q., Su, J., Chung, T.-S., Amy, G. 2011, Hydrophilic Superparamagnetic Nanoparticles: Synthesis, Characterization, and Performance in Forward Osmosis Processes. Ind. Eng. Chem. Res. 50(1), 382-388.

Ling, M. M., Chung, T.-S., Lu, X. 2011, Facile synthesis of thermosensitive magnetic nanoparticles as "smart" draw solutes in forward osmosis. Chem. Commun. 47(38), 10788-10790.

Ge, Q., Su, J., Amy, G. L., Chung, T.-S. 2012, Exploration of polyelectrolytes as draw solutes in forward osmosis processes. Water Res. 46(4), 1318-1326.

Sarp, S., Lee, S., Park, K., Park, M., Kim, J. H., Cho, J. 2012, Using macromolecules as osmotically active compounds in osmosis followed by filtration (OF) system. Desalination and Water Treatment 43(1-3), 131-137.

373 Alnaizy, R., Aidan, A., Qasim, M. 2013, Draw solute recovery by metathesis precipitation in
374 forward osmosis desalination. Desalination and Water Treatment 51(28-30), 5516-5525.

375 Cai, Y., Shen, W., Loo, S. L., Krantz, W. B., Wang, R., Fane, A. G., Hu, X. 2013, Towards
376 temperature driven forward osmosis desalination using Semi-IPN hydrogels as reversible
377 draw agents. Water Res. 47(11), 3773-3781.

378 Cai, Y., Shen, W., Wang, R., Krantz, W. B., Faneb, A. G., Hu, X. 2013, CO_2 switchable dual
379 responsive polymers as draw solutes for forward osmosis desalination. Chem. Commun.
380 49(75), 8377-8379.

381 Ge, Q., Chung, T.-S. 2013, Hydroacid complexes: a new class of draw solutes to promote
382 forward osmosis (FO) processes. Chem. Commun. 49(76), 8471-8473.

383 Li, D., Zhang, X., Yao, J., Simon, G. P., Wang, H. 2011, Stimuli-responsive polymer
384 hydrogels as a new class of draw agent for forward osmosis desalination. Chem. Commun.
385 47(6), 1710-1712.

386 Li, D., Zhang, X., Yao, J., Zeng, Y., Simon, G. P., Wang, H. 2011, Composite polymer
387 hydrogels as draw agents in forward osmosis and solar dewatering. Soft Matter 7(21), 10048-
388 10056.

389 Li, D., Zhang, X., Simon, G. P., Wang, H. 2013, Forward osmosis desalination using polymer
390 hydrogels as a draw agent: Influence of draw agent, feed solution and membrane on process
391 performance. Water Res. 47(1), 209-215.

392 Ou, R., Wang, Y., Wang, H., Xu, T. Thermo-sensitive polyelectrolytes as draw solutions in
393 forward osmosis process. Desalination 318, 48-55.

394 Razmjou, A., Barati, M. R., Simon, G. P., Suzuki, K., Wang, H. 2013, Fast Deswelling of
395 Nanocomposite Polymer Hydrogels via Magnetic Field-Induced Heating for Emerging FO
396 Desalination. Environ. Sci. Technol. 47(12), 6297-6305.

397 Razmjou, A., Liu, Q., Simon, G. P., Wang, H. Bifunctional Polymer Hydrogel Layers As
398 Forward Osmosis Draw Agents for Continuous Production of Fresh Water Using Solar
399 Energy. Environ. Sci. Technol. 47(22), 13160-13166.

400 Razmjou, A., Simon, G. P., Wang, H. 2013, Effect of particle size on the performance of
401 forward osmosis desalination by stimuli-responsive polymer hydrogels as a draw agent.
402 Chem. Eng. J. 215, 913-920.

403 Zeng, Y., Qiu, L., Wang, K., Yao, J., Li, D., Simon, G. P., Wang, R., Wang, H. 2013,
404 Significantly enhanced water flux in forward osmosis desalination with polymer-graphene
405 composite hydrogels as a draw agent. Rsc Adv. 3(3), 887-894.

406 Wang, H., Wei, J., Simon, G. P. Response to Osmotic Pressure versus Swelling Pressure:
407 Comment on "Bifunctional Polymer Hydrogel Layers As Forward Osmosis Draw Agents for
408 Continuous Production of Fresh Water Using Solar Energy". Environ. Sci. Technol. 48(7),
409 4214-4215.

410 Hartanto, Y., Yun, S., Jin, B., Dai, S. 2015, Functionalized thermo-responsive microgels for
411 high performance forward osmosis desalination. Water Res. 70, 385-393.

412 Zhang, H., Li, J., Cui, H., Li, H., Yang, F. 2015, Forward osmosis using electric-responsive
413 polymer hydrogels as draw agents: Influence of freezing–thawing cycles, voltage, feed
414 solutions on process performance. Chem. Eng. J. 259, 814-819.

415 Ali, W., Gebert, B., Hennecke, T., Graf, K., Ulbricht, M., Gutmann, J. S. 2015, Design of
416 Thermally Responsive Polymeric Hydrogels for Brackish Water Desalination: Effect of

417 Architecture on Swelling, Deswelling, and Salt Rejection. ACS Appl. Mater. Interfaces, 7,
418 15696-15706.

419 Liu, K., Ovaert, T. C., Mason, J. J. 2008, Preparation and mechanical characterization of a
420 PNIPA hydrogel composite. J. Mater. Sci.: Mater. Med. 19(4), 1815-1821.

421 Teramoto, N., Shigehiro, O., Ogawa, Y., Maruyama, Y., Shimasaki, T., Shibata, M. 2014,
422 Polymer foam-reinforced hydrogels inspired by plant body frameworks as high-performance
423 soft matter. Polym. J. 46(9), 592-597.

424 Wack, H., Ulbricht, M. 2009, Effect of synthesis composition on the swelling pressure of
425 polymeric hydrogels. Polymer 50 (9), 2075-2080.

426

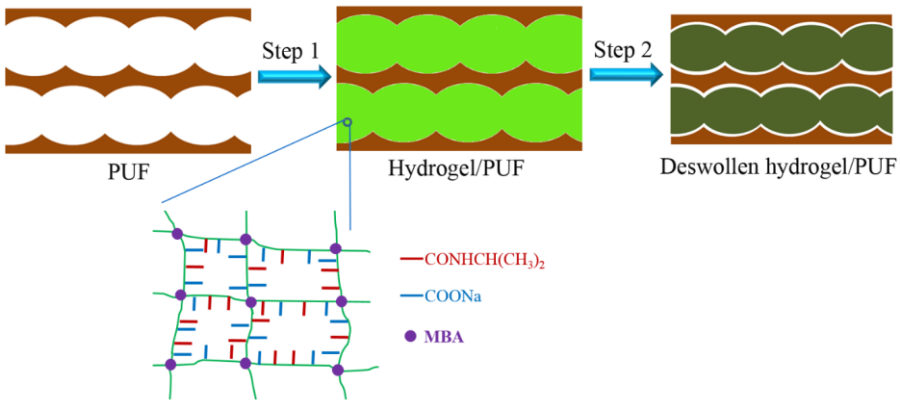

427

428 **Figure 1** Schematic of the preparation of dry hydrogel/PUF composites: Step 1,
429 polymerization of monomers in the matrix of polyurethane foam (PUF) to obtain the
430 hydrogel/PUF composites; Step 2, the removal of unreacted monomers and water via
431 washing and dry process.

432

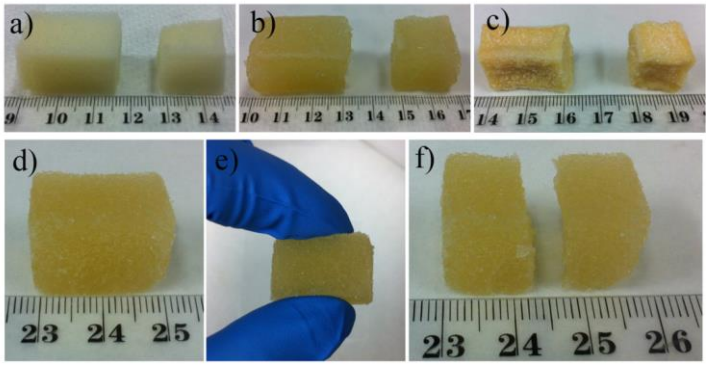

Figure 2 Photographs of a) polyurethane foam (PUF), b) after loading with PSA-*co*-PNIPAM hydrogel, c) dry hydrogel/PUF composites, d) hydrogel/PUF before being cut, e) hydrogel/PUF held with fingers, and f) hydrogel/PUF after being cut with scissors.

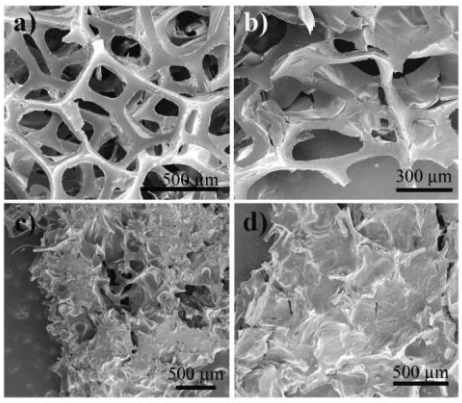

Figure 3 Scanning electron microscopy (SEM) images of a) PUF, b)dry Hydrogel/PUF-1:1, c) dry Hydrogel/PUF-3:1, and d) dry Hydrogel/PUF-8:1.

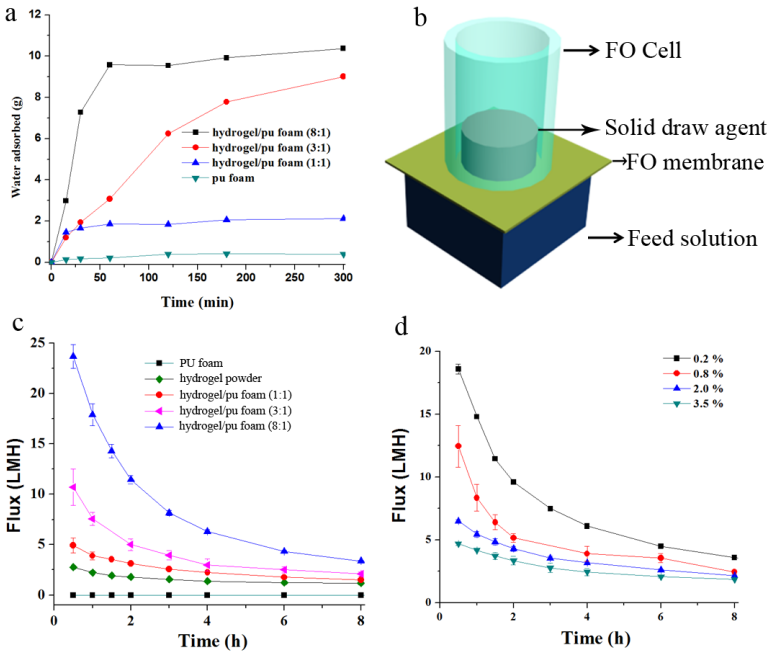

Figure 4 a) The swelling experiment, which was carried out by soaking the monolith with the same size (about 1×1×1.5 cm) in 500 ml of DI water. b) The schematic for the forward osmosis (FO) desalination process by using the hydrogel as a draw agent. c) The flux measured by using hydrogel/sponge composites with different mass ratios as draw agent, and water as feed solution. d) The flux measured by using dry hydrogel/sponge composites (mass ratio of 8:1) as draw agent, and NaCl solution with different concentrations (0.2 - 3.5 wt%) as the feed solution.

Commented [HW1]: Revise this, which is not consistent with Fig 4a. Also the font sizes are too small.

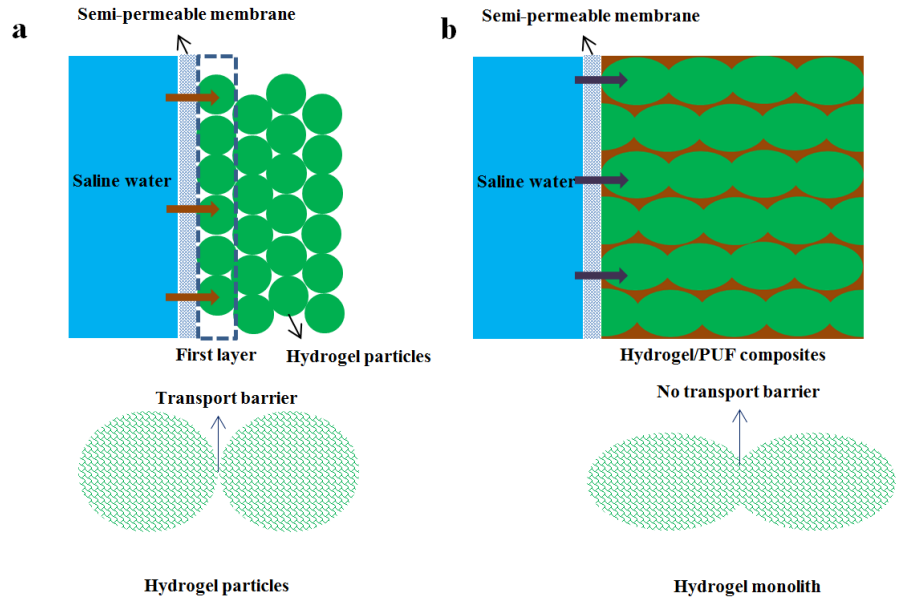

Figure 5 Water transport in the (a) hydrogel powder and (b) hydrogel/PUF composite.

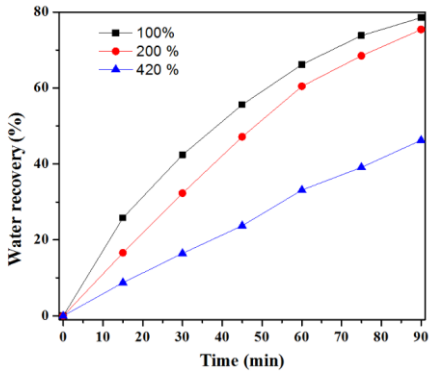

Figure 6 Water recovery of hydrogel/PUF composites with different swelling ratios (100, 200 and 420 wt%) under concentrated, simulated solar irradiation (2 kW/ m^2).

Supporting information

Hydrogel-polyurethane Interpenetrating Network as an Advanced Draw Agent for Forward Osmosis Desalination

Jing Wei[1], Ze-Xian Low[1], Ranwen Ou[1], George P Simon[2], Huanting Wang[1]

[1]Department of Chemical Engineering, Monash University, Clayton, Victoria 3800, Australia
E-mail: huanting.wang@monash.edu
[2]Department of Materials Engineering, Monash University, Clayton, Victoria 3800, Australia

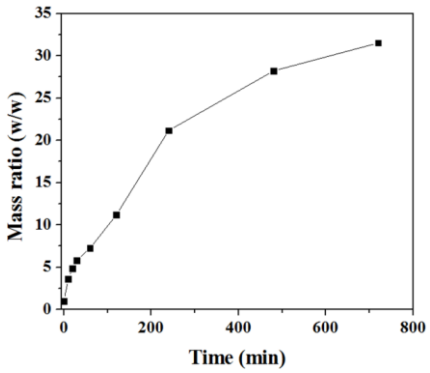

Figure S1 The swelling kinetic for the hydrogel-polyurethane interpenetrating network (HPIPN) in pure water.

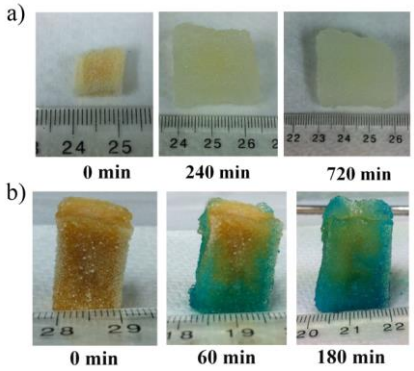

Figure S2 a) Photos of the hydrogel/PUF composites with different soaking times (0, 240 and 720 min) b) The hydrogel/PUF after standing within the copper nitrate solution, to test water transport in the composite.

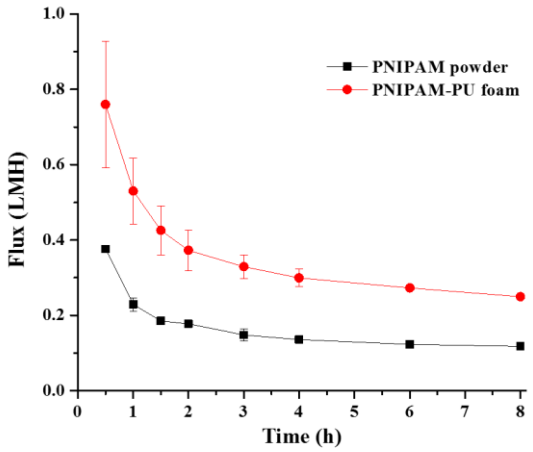

Figure S3 The flux measured by using PNIPAM hydrogel/sponge composites and PNIPAM hydrogel powders as draw agent, and water as feed solution.

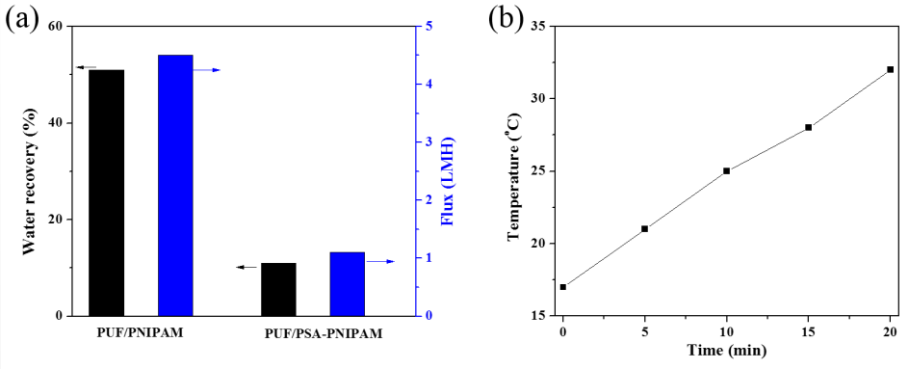

Figure S4 (a) Water recovery and dewatering flux of PUF/hydrogel composites with swelling ratio of 350 % (Black: PUF/PNIPAM; Blue: PUF/PSA-PNIPAM) after heating for 20 min. (b) The temperature of PUF/PSA-PNIPAM versus time under heating.

Commented [HW1]: Please specify heating condition. Solar heating under 2 kW/m2??

Commented [HW2]: ??

Table S1 Summary of the FO flux using polymer hydrogels and their composites as the draw agents

Materials	1h's Flux (LMH)	Feed Solution	Reference
PSA	0.96	0.2 wt% NaCl solution	1
PNIPAM	0.27	0.2 wt% NaCl solution	1
PNIPAM-*co*-SA (size of 2-25 μm)	1.0	0.2 wt% NaCl solution	2
PSA/Carbon	1.06	0.2 wt% NaCl solution	3
PSA/rGO	3.1	0.2 wt% NaCl solution	4
PSA-co-PNIPAM/rGO	1.7	0.2 wt% NaCl solution	4
PSA-co-PNIPAM/γ-Fe_2O_3	1.4	0.2 wt% NaCl solution	5
PNIPAM-SA (semi-IPN)	0.24	0.2 wt% NaCl solution	6
Microgel (PNIPAM)	2	0.2 wt% NaCl solution	7
Microgel (PNIPAM-PAA)	4	0.2 wt% NaCl solution	7
PSA-*co*-PNNIPAM-PUF	14.8	0.2 wt% NaCl solution	This study

References

1. Li, D., Zhang, X., Yao, J., Simon, G. P., Wang, H. 2011, Stimuli-responsive polymer hydrogels as a new class of draw agent for forward osmosis desalination. Chem. Commun. 47(6), 1710-1712.

2. Razmjou, A., Simon, G. P., Wang, H. 2013, Effect of particle size on the performance of forward osmosis desalination by stimuli-responsive polymer hydrogels as a draw agent. Chem. Eng. J. 215, 913-920
3. Li, D., Zhang, X., Yao, J., Zeng, Y., Simon, G. P., Wang, H. 2011, Composite polymer hydrogels as draw agents in forward osmosis and solar dewatering. Soft Matter 7(21), 10048-10056
4. Zeng, Y., Qiu, L., Wang, K., Yao, J., Li, D., Simon, G. P., Wang, R., Wang, H. 2013, Significantly enhanced water flux in forward osmosis desalination with polymer-graphene composite hydrogels as a draw agent. Rsc Adv. 3(3), 887-894.
5. Razmjou, A., Barati, M. R., Simon, G. P., Suzuki, K., Wang, H. 2013, Fast Deswelling of Nanocomposite Polymer Hydrogels via Magnetic Field-Induced Heating for Emerging FO Desalination. Environ. Sci. Technol. 47(12), 6297-6305
6. Cai, Y., Shen, W., Loo, S. L., Krantz, W. B., Wang, R., Fane, A. G., Hu, X. 2013, Towards temperature driven forward osmosis desalination using Semi-IPN hydrogels as reversible draw agents. Water Res. 47(11), 3773-3781
7. Hartanto, Y., Yun, S., Jin, B., Dai, S. 2015, Functionalized thermo-responsive microgels for high performance forward osmosis desalination. Water Res. 70, 385-393.